Korean J. Chem. Eng., **28**(8), 1641-1650 (2011)
DOI: 10.1007/s11814-011-0183-5

INVITED REVIEW PAPER

Synthesis and assembly of anisotropic nanoparticles

Gaehang Lee*, Young-Sang Cho, Sungkyun Park***, and Gi-Ra Yi****,†**

*Division of Materials Science, Korea Basic Science Institute, Daejeon 305-806, Korea
**Department of Powder Materials, Korea Institute of Materials Science, Changwon, Gyeongnam 641-831 Korea
***Department of Physics, Pusan National University, Busan 609-735, Korea
****Department of Engineering Chemistry, Chungbuk National University, Cheongju, Chungbuk 361-763 Korea
(*Received 18 July 2011 • accepted 22 July 2011*)

Abstract−Unifrom nanoparticles with shape-anisotropy have been synthesized successfully, including rod-like, disk-like (or platelet), or faceted nanoparticles. Recently, innovative methods for funtionalizing their surfaces anisotropically have been devised, which involve site-selective attachment of organic ligands or nanoparticles on particle surface. Those techniques have opened a new way to build up complex nano-architectures by self-assembly. Moreover, recent progress in the synthesis and assembly of anisotropic colloids at micrometer scale has inspired directional self-assembly at nano-scale with anisotropic nanoparticles, which could lead to various nanodevices with better performance. In this review, we discuss synthetic methodology for anisotrpic nanoparticles, including nanorods, nanoplatelet (or nanodisks), faceted nanoparticles and hybrid nanoparticles. Their opitical properties and self-assembled structures are also discusssed.

Key words: Anisotropy, Nanoparticle, Self-assembly, Colloids, Nanoarchitecture

INTRODUCTION

For the last few decades, novel physical or chemical properties of nanoparticles have been investigated that are different from bulk materials and unique because of their feature size at nanometer scale and diverse shape. Thus far, many researchers have focused on developing efficient methods for making nanometer-sized particles. In the meantime, new physical or chemical properties, which are not discovered yet, have been pursued by analyzing synthesized nanoparticles in many different ways, including theoretical investigation. Recently, controlling size distribution or shape has been a new issue in this research field and much effort been put on this problem. Therefore, technological achievement has almost matured in terms of making nanoparticles with controlled size which have many promising properties as in previous reports [1-5]. On the other hand, for enabling new functions to work in real devices, their assembled structures have been investigated, in which optimal structure has been pursued for better device performance. For instance, solar cells with nanorods have been proposed as the most efficient light conversion devices. Rod-like semiconducting nanoparticles have been implemented with conducting polymers. However, their performance (power conversion efficiency ~2%) has not been higher than expected compared to conventional devices or bulk structures because nanorod structures are more or less random and not optimized [1]. Recently, to resolve such issue in nanodevices including nanoparticle-based solar cells, many research groups have tried to guide self-assembled structure with top-down manufacturing techniques. In most cases, well-defined pre-existing structures by top-down fabrication process have been used for guiding the self-assembly of nanoparticles. However, these pre-fabricated structures are limited to very small area and also require time and cost. From the industrial point of view, assembling process should be less complicated and productivity should be high or at least similar compared to the one of the current fabrication process.

Therefore, innovative methodology has been required for this research field. One candidate is the synthesis of nanoparticles with controllable and directional interaction. Self-assembly of those nanoparticles, or directional self-assembly, will provide much more cost-effective manufacturing strategy for many useful nanodevices, including sensors, photonic circuits, optoelectronic devices and so on.

To this end, it is necessary to design, synthesize and functionalize the nanoparticles since the most of nanoparticles developed so far were isotropic particles. Notably, it is important that intrinsic function or properties of nanoparticles should not be degraded during functionalization or assembling process. Recently, Glotzer and Solomon have categorized few types of anisotropic particles at micrometer and nanometer scale which are desirable for new structures and they summarized some examples reported in previous articles [2]. Anisotropic micron- or submicron-sized particles have been reviewed in several articles [3]. Here, we have focused on anisotropic particles at nanometer scale and also their anisotropic interaction which is crucial for directional self-assembly. In particular, the physical properties of newly synthesized anisotropic particles or their combined structures will be reviewed. Furthermore, recent progress on their self-assembled structure and potential applications will be also discussed.

SYNTHESIS OF ANISOTROPIC NANOPARTICLES

Since nanoparticles are known to have new physical and/or chemical properties, much research effort has been endeavored to produce nanometer-size particles at initial stage. Then, recently, some strategies for controlling the size distribution have been demonstrated

†To whom correspondence should be addressed.
E-mail: yigira@chungbuk.ac.kr

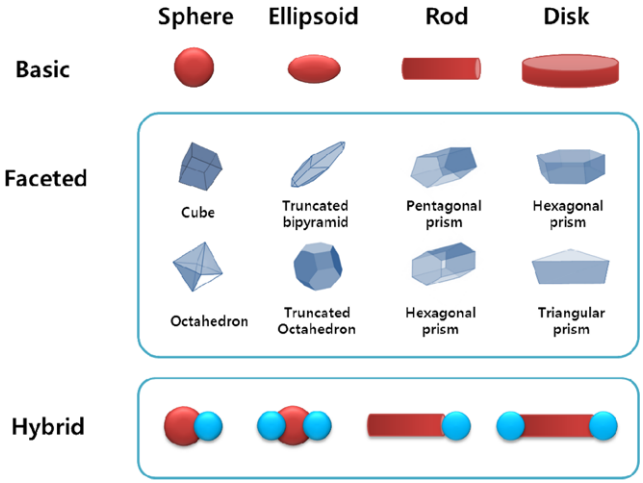

Scheme 1. Schematic diagram of anisotropic nanoparticles with basic (top), faceted (middle) and hybrid shape (bottom).

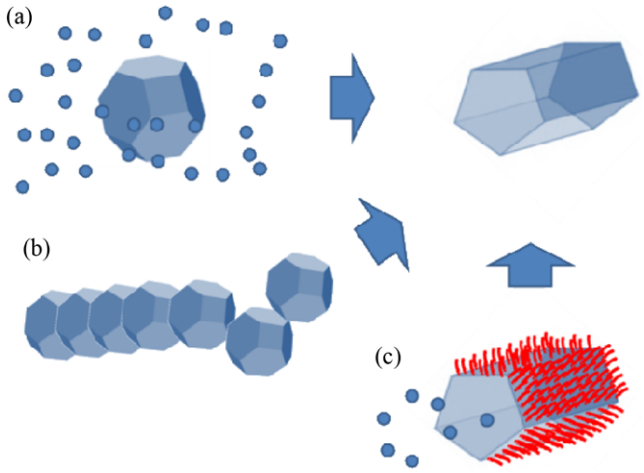

Fig. 1. Schematic diagram of (a) intrinsic crystallographic structure, (b) oriented attachment, and (c) selective adhesion of surfactant for rod-like nanoparticles.

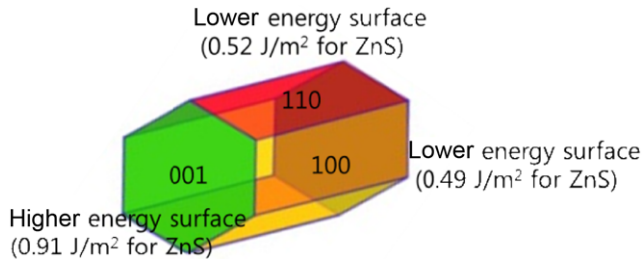

Fig. 2. Illustration of surface energy for wurtzite hexagonal phase [15].

for certain types of nanoparticles [4]. However, it is still relatively few for preparing anisotropic particles with narrow size distribution, which will be of critical importance in assembling them into three-dimensional structures. As summarized in Scheme 1, anisotropic nanoparticles of which feature size ranges from 1 nm to 100 nm can be categorized depending on their shapes.

1. Spherical and Ellipsoidal Particles

As in previous articles, spherical nanoparticles of various materials have been reviewed thoroughly [4] and their assembled structures are well-known to be close-packed structures. By stretching or squeezing spherical shape, micron-sized ellipsoidal colloids could be produced but ellipsoidal nanoparticles are relatively few. Only for metal oxides, a few ellipsoidal nanoparticles have been, which includes iron oxide, titania [5]. Using those as templates, hollow particles of silica were produced and modified for other purposes [6]. For metallic particles, ellipsoidal particles are very unusual because most metallic particles are crystalline structure, thus not compatible with round shape. Similar to spherical metallic particles which are essentially multi-twinned particles, some truncated bipyramid metallic particles are overall ellipsoidal shapes as shown in Scheme 1 [7].

Another type of anisotropic particle from spheres would be decoration with the other spherical nanoparticles. As shown at the bottom of Scheme 1, a single particle or multiple particles can be grown on spherical particles. Iron oxide nanoparticles were decorated with gold nanoparticles [8], and Pd nanoparticles were also decorated with platinum nanoparticles [9]. Xu et al. have also demonstrated iron platinum nanoparticles with CdS [10]. Acron-shaped bimetallic particles were also produced by Sano et al. [11]. Gold nanoparticles were also decorated with iron oxides [12].

2. Rod-like Particles

For crystalline materials, the growth ratio of crystal plane, which is considerably related to interaction between a surface atom and organic molecule, plays a critical factor in determining morphology of a nanostructure. The stronger the binding is of a surfactant to on-growing crystal plane atom, the slower the growth rate of the surface direction become. Consequently, a fast-growing crystal plane disappears gradually as a reaction proceeds and a plane with relatively slow growth becomes the outer surface plane of a final nanoparticle.

When the aspect ratio (a.r.) of nanoparticles is a.r.<5, 5<a.r.<25, or a.r.>25, corresponding particles are classified as short nanorods, long nanorods, or nanowires, respectively [13]. The general strategies for the nanorods in liquid phase are to use intrinsic crystallographic structure, oriented attachment, or selective adhesion of surfactant (Fig. 1) [14].

In case of using intrinsic crystallographic structure, an inorganic compound should have asymmetric surface energy. For instance, CdS, CdSe, CdTe, ZnSe, and MnS are a hexagonal wurtzite structure. As shown in Fig. 2, the surface energy of {001} face in wurtzite structure is higher than that of the other faces because of high packing density [15].

Using this surface energy difference between crystallographic surfaces, the CdSe nanorods were synthesized by simply adding precursors in solvent above the decomposition temperature of precursors, in which 2 ml of stock solution (Se : $Cd(CH_3)_2$: tributylphosphine=1 : 2 : 38 by weight) were added into 4 g of trioctylphosphine oxide at 360 °C [16]. Agostiano et al. demonstrated that ZnSe nanorods can be synthesized in similar manner, in which the aspect ratio was also controlled by changing injection rate [17]. On the other hand, tetragonal phase could be also controlled because it has the high surface energy of {001} plane. For instance, the TiO_2 and

Mn_3O_4 nanostructures were produced by heating the solution containing metal chloride, oleic acid, and oleylamine [18]. This techique has been also applied to other strucures [19].

In case of the oriented attachment for the nanorods, the particles undergo fusion at preferential crystallographic surfaces. For example, cubic ZnS nanorods were formed by the oriented attachment of ZnS nanoparticles [20]. Zn precusor was injected into a solution containing sulfur element and 1-hexadecylamine at 125 ºC, followed by heating at 300 ºC. ZnS nanoparticles were gradually transformed into rod during the aging process at 60 ºC [20]. Recently, oriented attachment of ZnO nanoparticles was also observed by Weller and his colleagues. At first, the quasi-spherical particles were formed by zinc acetate dihydrate dissolved in methanol at about 60 ºC and then KOH in methanol was added into ZnO particle suspension. Subsequently, during the evaporation of the solvent and then reflux of the resulting solution, rod-shaped particles were produced [21], in which charges on primary nanoparticle surface may play an important role in formation of ZnO nanorods. Yang et al. also reported the surfactant-free ceria nanorods by self-assembly of the nanocrystals [22], in which nanorods were formed by injection of NaOH aqueous solution into $Ce(NO_3)_3$ aqueous solution and refluxing the resulting solution at 100 ºC.

For selective adhesion of surfactant, after seed formation, organic molecules, strongly bind to specific crystal plane (e.g., high surface energy), provide kinetic control to extend along one-direction upon growing of the nanostructures [23]. Liu et al. reported that addition of serial growth aqueous solution with gold precursor ($HAuCl_4$) into the gold seed solution at 30 s intervals created Au nanorods [23]. The evolution of the Au nanorods by a serial addition of growth solution was investigated through X-ray absorption spectra. El-Sayed et al. have also shown that gold nanorods can be synthesized by seed-mediated growth [24], in which the Au seed solution is added into the growth solution. The silver ion and the surfactants played crucial role on controlling the aspect ratio of the gold nanorods. Murphy et al. demonstrated that the aspect ratio of gold nanorods can be also controlled by the injection sequence or amount of ascorbic acid or Ag ion for the Au growth solution [13].

On the end of rod-like particles, nanoparticles can be formed by selective overgrowth because of the surface energy difference or preferential adsorption of surfactant. For instance, PbSe were formed on either one or both tip of a CdS nanorod due to the surface energy difference among various facets of wurtzite nanorods [25]. Similarly, gold nanoparticles were formed onto the tips of CdSe nanorods and tetrapods [26]. On the other hand, Li et al. have recently reported that hexagonal pyramid of ZnO can be grown on spherical gold nanoparticles [27].

3. Nanoplate Particles

In most cases of metals, plate-like particles are synthesized by selective growth due to adsoprtion of surfactant or engery difference of crystallographic surface on seed particles with stacking faults. Xia et al. demonstrated the silver nanoplates made from slow polyol reduction of $AgNO_3$ [28]. The amino groups of polyacrylamide as surfactant form a complex with Ag^+ ion. This interaction led to decreaseed reducing rate of silver precursor into Ag metal. Also, the kinetic control employing the molar ratio of the sodium citrate and poly(vinyl pyrrolidone) gave rise to synthesis of the single crystalline gold nanoplates [29].

Silver nanoplates have been also produced during seeded growth of silver nanoparticles by photo-reduction process, in which light at 457 nm was irradiated at 0.8 W/m^2 and Ag nanoparticles were transformed into disk type. The citrate ion may be adsorbed on the Ag seed surface and then act as a surfactant as well as a photoreducing agent for the silver ions, thereby producing the Ag nanodisk [30].

In the case of metal oxide, Cao reported a colloidal synthesis of square, plate-shaped gadolinium-oxide nanocrystals [31]. Gd_2O_3 nanoplates were synthesized by solvothermal decomposition of the mixture solution containing gadolinium acetate hydrate, oleylamine, oleic acid, and octadecene. To form plate shape, the combination of three solvents (oleylamine, oleic acid, and octadecene) plays a key role. Using selective adsorption of co-surfactants (oleic acid and oleylamine) on specific crystal planes, Yan et al. created rare-earth oxide nanocrystals by solvothermal decomposition of rare-earth metal benzoylacetonate complexes in oleic acid and oleylamine [32]. Uniform disk- or plate-like nanoparticles of Cu_2S were also demonstrated by thermolysis. Those platelets are self-assembled into column-like stacks, which was induced by Tin [33].

4. Faceted Particles

As described earlier for rod-like particles, facets of crystalline metal nanoparticles can be controlled. In most cases, surfactant or ions are bound on specific surfaces preferentially and growth rate is suppressed. Thereby, we can make faceted nanoparticles which have specified crystallographic planes bounded with surfactant. Huang et al. demonstrated that the octahedral Au nanoparticles could be formed by hydrothermal reaction in presence of surfantant (CTAB) and they controlled their size by reaction time [34]. Intrinsic growth rates of faceted nanoparticles is different along crystallographic direction. In case of octahedra, when {100} growth rate is much fast than that of {111}, octahedal shape forms as depicted in Fig. 3. If ion or surfactant are bound on {100} plane, cubes can be formed from octahedra. General synthetic methodology for faceted metallic particles using surface engergy of crystallographic plane or preferential adsorption of surfactant or ions has been reviewed by Xia and the others thoroughly [19].

The size of the nanoparticles has gradually increased as the reaction temperature increases. Cho et al. reported the uniform tailorable-size gold octahedral [36]. The particles were obtained by polyol synthesis in a glass vial containing poly(diallyldimethylammonium) chloride (PDDA), HCl, aqueous $HAuCl_4$, and ethylene glycol. The PDDA among the reactants plays a crucial role in the formation of

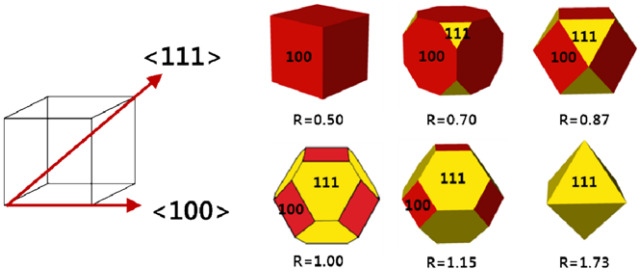

Fig. 3. Schematic model for the various shape of a nanostructures depending on the ratio (R) of the growth rate along <100> to <111> [35].

octahedra shape. Also, the decrease of reduction rate creates larger Au octahedra. Yang et al. demonstrated that silver cubes, truncated cubes, cuboctahedra, truncated octahedra, and octahedra can be synthesized in one reaction system [37]. Silver nitrate and copper(II) chloride were dissolved separately in 1,5-pentanediol. Poly(vinylpyrrolidone) (PVP) was dissolved separately in 1,5-pentanediol. The two kinds of solution were injected into the preheated pentanediol. The polyhedral shapes depend on the amounts of the added reactants into the hot solution.

In addition to an octahedra, FePt nanocube could be produced by elaborately controlling the reaction temperature. The FePt particles were produced in thermal decomposition of $Pt(acac)_2$ and $Fe(CO)_5$ dissolved in oleic acid, benzyl ether, and octadecene [38]. The silver mirror reaction, addition of *n*-hexadecyltrimethylammonium bromide into aqueous $[Ag(NH_3)_2]^+$ solution, forms the nanocube [39].

The morphology of the particles could be tuned by controlling the ratio of reduction rate of two different precursors at the nucleation and growth stages. For instance, when two types of precursors for platinum, $(NH_4)_2Pt(IV)Cl_6$ and $(NH_4)_2Pt(II)Cl_4$) are used for platinum nanoparticles, and particle morpholgoy or size can be controlled precisely by adjusting reduction rate in nucleation and growth stages, which depends on concentration ratio of Pt(II) to Pt(IV). Indeed, morphology or size of platinium particles could be controlled precisely at sub 10-nanometer scale. In particular, when Pt(II) was less than Pt(IV), the smaller nanocubes were produced well because the reduction rate of Pt(IV) ion is slower than that of Pt(II) ion during growth stage [40].

Recently, Lee and colleagues have described current progress on synthetic methodology for controlling faceted nanoparticles, which is etching assisted kinetic and thermodynamic control, metal doping-induced kinetic and thermodynamic control, high energy surface stabilization by small molecules or ions, and epitaxial growth [41]. Currently, other types of faceted particles are under investigation based on method discussed above or new methods are under development.

OPTICAL PROPERTIES OF ANISOTROPIC NANOPARTICLES

One of the interesting physical properties of nanoparticles that originated from their shape-anisotropy is the optical property of metal nanoparticles with nonspherical morphologies and their self-assembled architectures. For instance, anisotropic metallic nanoparticles possess anomalous extinction spectrum according to their shapes and these optical resonance phenomena can be applied for sensing or waveguiding purposes. This section will focus on the review of optical properties of metal nanoparticles with anisotropic shapes. The optical resonance of multi-nanoparticle assemblies, namely *plasmonic molecules* or *plasmonic crystals*, will be also reviewed in the light of novel architectures by self-assembly.

1. The Origin of Surface Plasmon Resonance from Metal Nanoparticles

Since Faraday's scientific research on the brilliant colors of gold nanoparticles, the light scattering or absorption from metal nanoparticles has attracted much attention due to the size-dependent optical extinction of zero-dimensional nanoparticles. As an early achievement of classical electromagnetic theory, Mie obtained exact solution to Maxwell's equations for the predictions of the optical spectrum of spherical metal nanoparticles in analytic fashion. The concept of Mie scattering could be used as useful theoretical background for the comparison of experimentally obtained absorption spectrum of metal nanoparticles such as gold or silver.

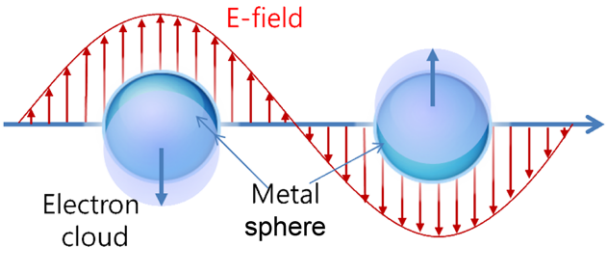

Fig. 4. Schematic diagram for the coherent oscillation of electrons for metallic sphere [42].

Nowadays, the light extinction phenomenon from metal nanoparticles is explained by using the concept of *surface plasmon resonance* (SPR), of which the term implies collective oscillation of electrons within metal surfaces. When an external electromagnetic field exists near metal particles having diameter much smaller than the wavelength of the external field, the electron cloud oscillates coherently and the induced charge oscillation can be confined or enhanced on the surface of the matal nanoparticles as displayed in Fig. 4 [42]. This localized charge oscillation is called localized surface plasmon resonance (LSPR), and this collective oscillation results in the scattering and absorption of light at particalular frequency. Thus, colloidal metal nanoparticles reveal brilliant colors of purple or yellow for gold or silver, respectively.

During the last decade, various synthesis methods were successfully developed for the morphology control of metal nanoparticles with the aids of various wet colloid chemistry. As explained in detail previously, besides spherical particles, anisotropic metal nanoparticles such as rods, triangles, cubes, and bipyramids can be synthesized at laboratory scale. The optical extinctions of anisotropic metal nanoparticles have been studied both experimentally and theoretically, which will be highlighted.

2. Optical Properties of Anisotropic Metal Nanoparticles-theoretical Approaches

The most simple nanostructures deviated from spheres are ellipsoidal particles such as oblates or prolates and the light extinction from these ellipsoidal nanostructures can be predicted by the modified version of Mie's theory proposed by Gans [43]. Moreover, the collective behavior of the nanostrucures such as nanoparticle-embedded films can be also theoretically treated by effective medium theory which was developed by Maxwell-Garnett and Bruggemann for the composite media with varying amounts of infiltrated materails [44,45]. The theoretical prediction for nanospheres, prolates, and glass films loaded with gold nanospheres coincided well with experimentally measured extinction spectra [46]. Interesting features can be found for the extinction spectrum of the prolate particles especially for the easy controllability of peak wavelength in the extinction spectrum by changing the aspect ratio of the anisotropic particles. Since the increase of the aspect ratio of prolate particles leads to the red-shift of the main peak, the effect of morphological change of anisotropic particles is more pronounced than the case of isotro-

pic gold nanospheres. Moreover, since the longitudinal surface plasmon absorption (SPL) and the transverse surface plasmon absorption (SPT) coexist for the prolate gold ellipsoidal particles in the extinction spectrum due to the random orientation of the anisotropic particles with long and minor axes due to Brownian motion in colloidal state, two absorption modes can be found together [46].

Since Mie's scattering theory can be applied only to spherical morphologies, several computational schemes have been developed for the predictions of the optical extinction from shape-anisotropic nanoparticles. The following schemes are numerical methods for the description of nonspherical metal nanoparticles.

(1) Discrete dipole approximations (DDA) [47]
(2) Multiple multipole methods (MMP) [48]
(3) Finite-difference time-domain (FDTD) methods [49]
(4) T-matrix methods [50]

Among those approaches, the DDA method is widely used for the optical characterizations of anisotropic nanoparticles with less computational difficulty, since the DDA calculation can predict the SPR of nonspherical metal nanoparticles and the complex external environments can be reflected during the simulation. Any arbitrary shaped nanostructures can be sub-divided into small elements (usually larger than 2 nm in characteristic length scale) with dipole-dipole interactions followed by the global evaluation for absoprtion and scattering during DDA simulations. Finally, the optical extinction from the nonspherical nanostructures can be obtained theoretically and the results can be compared with the experimentally measured spectrum from synthesized anisotropic metal nanoparticles. Fig. 5 shows the calculated spectrum of extinction from metal nanoparticles made of silver with various morphologies [51].

Since anisotropic nanoparticles possess several types of distinct symmetries, more than one unlike spherical particles, there is more than one peak in the optical extinction spectrum of nanoparticles as

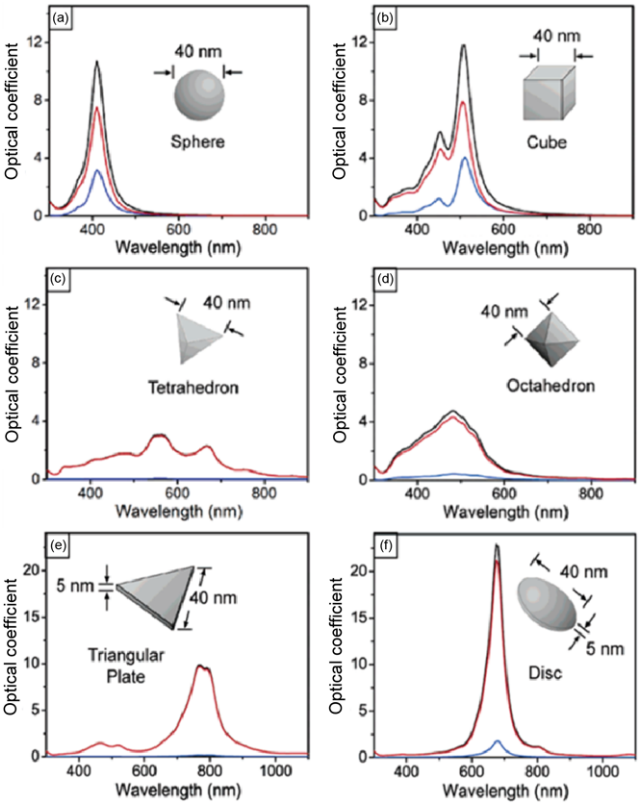

Fig. 5. Calculated UV-vis spectrum of anisotropic metal nanoparticles - extinction (black), absorption (red), scattering (blue) - obtained by DDA calculations. The anisotropic morphologies are (a) sphere, (b) cube, (c) tetrahedron, (d) octahedron, (e) triangle and (f) disk. The feature size of each nanostructure is 40 nm [51]. Reprinted with permission from ref. 51 Coppright 2006 American Chemical Society.

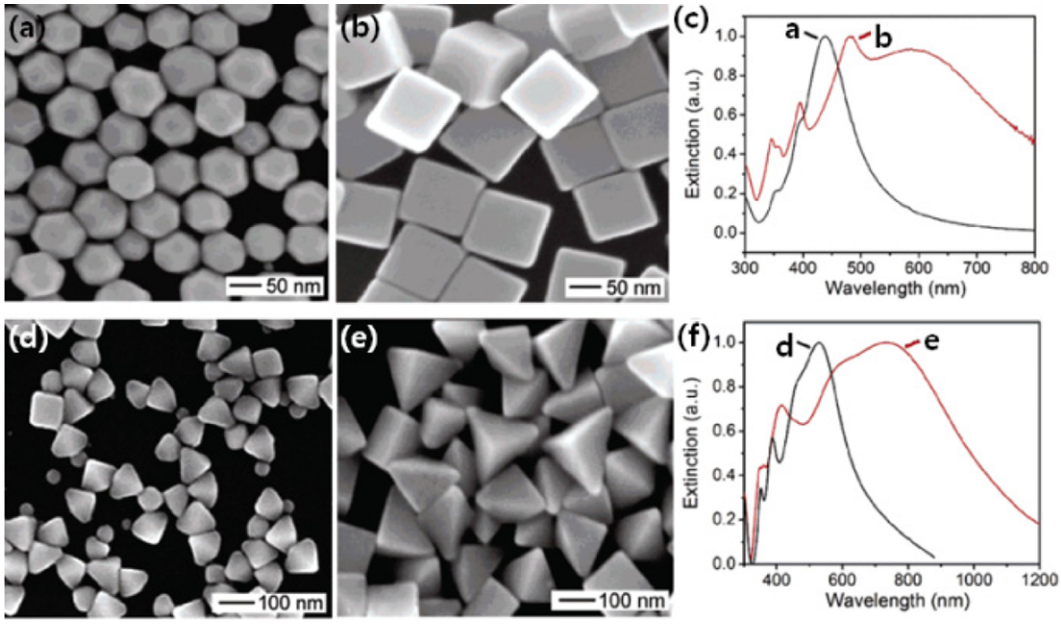

Fig. 6. (a) and (b) SEM image of nanocubes with truncated and sharper corners, respectively. (c) UV-vis extinction spectrum of the cubic nanoparticles. (d) and (e) SEM image of bipyramid nanoparticles with truncated and sharper corners, respectively. (f) UV-vis extinction spectrum of the bipyramidal nanoparticles [51,56,58]. Reprinted with permission from ref. 51, 56, 58 Copyright 2006, 2004, 2006 American Chemical Society.

displayed in Fig. 5(b) to (d). Besides the existence of the additional resonance peaks, the position of the main extinction peak from the nanostructures with sharp corner such as cube, tetrahedron, and octahedron can be red-shifted as shown in Fig. 5(b), (c), and (d). This is attributed to the charge accumulation near the sharp corners and the resultant reduced restoring force for electron oscillation [51].

Other anisotropic structures with 2D anisotropy were also considered for the prediction of extinction spectra by DDA calculations, as shown in Fig. 5(e), (f). Especially, the intensity of extinction peak can be also increased for the nano-disk shown in Fig. 6(f) since the effective dipole moment increases due to its circular symmetry for the nanostructures with round-shaped corners [51].

As a rule of thumb, the SPR properties of anisotropic nanoparticles can be summarized as follows:

(1) The increase of resonance frequencies by increasing the number of symmetries in the nanostructures;

(2) The red-shift of resoance wavelength with increased corner sharpness of the nanostructures;

(3) The increase of resonance intensity with an increase of mirror symmetry in the nanostructures.

3. Optical Properties of Anisotropic Metal Nanoparticles-Experimental Validations

Shape-anisotropic nanoparticles could be synthesized by lithographic techniques such as anodic aluminum oxide (AAO) membranes as templates. Martin and colleagues applied AAO templates for the deposition of gold inside the pores of the templates to synthesize gold cylinders with varying geometries, and the resultant extinction spectra could be measured with direction perpendicular to the long axis of gold nanocylinders [52]. Their measurements were extended by changing the direction of the incident light to the gold cylinders to observe the angle-dependent optical extinction spectrum [53]. Unlike gold nanorods suspended in liquid dispersion, the AAO-templated gold nanocylinders could be aligned into specific directions, thus enabling the control of the angle between the incident light and the direction of the long axis of the nanocylinders.

For gold nanorods by solution chemistry, surface plasmon peak wavelength were also measured as a function of their aspect ratio [54,55]. The surface plasmon longitudinal wavelength was compared with the theoretical results predicted by using Gans formula. Though there is some discrepancy between the measured and the predicted values, the theory coincides well with the experiments, especially for the red-shift trends with increasing aspect ratio of nanorods.

Fig. 6 contains the TEM images of anisotropic silver nanoparticles with more complex morphologies rather than nanorods and their resultant UV-vis extinction spectrums. For the truncated nanocubes shown in Fig. 6(a), NaCl was added to the seed particles for the oxidative etching and formation of truncated morphologies. For the sharper silver nanocubes in Fig. 6(b), HCl was added for the suspension of seed particles [56,57]. Although both anisotropic particles revealed multiple extinction peaks, truncated particles exhibited extinction spectrums closer to the spherical silver nanoparticles, as displayed in the extinction spectrum of Fig. 6(c). Similar behaviors were also observed by changing the shape-controlling agent with NaBr instead of NaCl, and the reaction time was controlled as 3 and 5 hours to synthesize silver bipyramidal nanoparticles with edge length of 75 and 150 nm, respectively, as displayed in the TEM images of Fig. 6(d) and (e) [58]. Though both bipyramidal silver nanoparticles exhibited multiple extinction peaks, the larger anisotropic nanoparticles revealed the red-shift of the main resonance peak into near infrared region, compared to the extinction spectrum of the silver nanocubes (see the extinction spectrum of Fig. 6(f)). For the case of nanowires, the seed particles can be grown into the high aspect ratio structures by adding the iron ions for the prevention of the etching during the reaction. The reaction time could be controlled from 30 to 60 min to adjust the length of the silver nanotubes with 150 nm and micron-scale, resepectively [59,60]. After the complete growth of the silver nanowires, the extinction spectrum became more sharper due to the increased charge separation along the nanowire structures [54].

4. Chemical Sensors Based on Anisotropic Nanoparticles

Since surface plasmon resonance of anisotropic metal nanoparticles can be tuned by changing the morphologies of the nanostructures and their surrounding environments, they can be used for various sensing applications: for instance, surface plasmon resonances of silver nanoprisms are much more sensitive than conventional silver nanospheres when the surrounding dispersion medium is changed, as shown in the optical absorption spectrum of silver nanoprisms with lateral dimensions of 80 nm (blue) and 60 nm (red) in Fig. 7 [61,62]. When the dispersion medium is changed with DMF (dotted), ethanol (dashed), and water (solid lines), the main peak positions of the absorption spectrums were changed as 657, 627, and 618 nm, respectively, for the case of silver nanoprisms with lateral dimension of 80 nm. However, the position of surface plasmon resonance was almost maintained albeit the dispersion medium was changed for the case of ordinary silver nanospheres. Thus, anisotropic nanoparticles can be applied for the detection of chemicals by measuring the surface plasmon resonance spectrums.

Besides sensors for chemical solvents, anisotropic nanoparticles can be applied as biosensors to detect biomolecules such as hemoglobins [63]. Jiang and colleagues synthesized gold nanorods with aspect ratio of 3.1 and performed silica coating for the formation

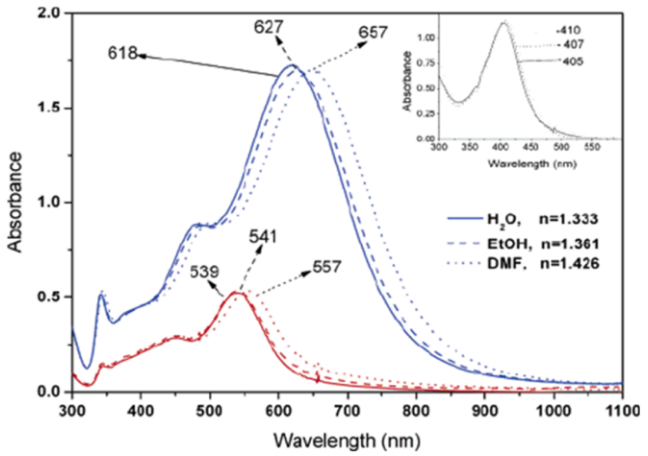

Fig. 7. Absorption spectrum of silver nanoprism with lateral length of 80 nm (blue) and 60 nm (red) under various environments of dispersion medium such as DMF, ethanol, and water [61, 62]. Reprinted with permission from ref. 61, 62 Copyright 2002, 2006 American Chemical Society.

of thin silica shell on the gold nanorods by sol-gel process. Then, hemoglobin molecules were adsorbed onto the gold nanorods and the resultant changes of absorbance spectrum were observed. The effect of silica coating on the change of absorption band was negligible, while the adsorption of hemoglobin led to the strong change of longitudinal plasmon band from 746 nm to 768 nm. Thus, anisotropic nanoparticles can be applied for the sensing applications of various chemicals as well as biomolecules.

5. Other Properties of Anisotropic Nanoparticles

Besides optical properties, other physicochemical properties can be expected for anisotropic nanostructures. For instance, the different magnetic properties between conventional nanoparticles (or nanospheres) and nanofibers have been measured, especially for the CoNi nanospheres and nanofibers, recently [64]. The first magnetization curve of CoNi nanofibers was measured with lower values compared to the value of CoNi nanospheres, possibly due to the orientation of the nanofibers on the demagnetizing field. Besides the first magnetization curve, the magnetorheological (MR) properties of the suspended CoNi nanofibers exhibited different behaviors other than the simple suspension of CoNi nanoparticles. The MR effect of nanofiber was considerably enhanced due to the higher yield stress of the nanofiber suspension.

ASSEMBLY OF ANISOTROPIC NANOPARTICLES

1. Packings of Anisotropic Nanoparticles

Because of shape-anisotropy, we can expect new types of self-assembled structures using anisotropic particles. Recently, Agarwal and Escobedo perfomed simulation and reported various types of self-assembled structure of polyhedral particles or faceted nanoparticles. Synthetic methods of some faceted nanoparticles were described earlier. By constrast, experimenal investigations of those structures are relatively few because those synthetic methods are relatively new and not popular so far. Moreover, it is very difficult to observe their self-assembly directly because they are too small for optical microscopy or it is very difficult to observe the intermediate state under electron microscopy. Nonetheless, there are a few reports on the self-assembled structure of faceted nanoparticles experimentally. Most of them are brief reports about simple observations of their local structures [34]. Yang and colleaques reported the self-assembled crystals of octahedal silver nanoparticles on large substrates by simple dip-coating method. Their plasmonic properties have also been studied [65]. They have tried to assemble cubic, cuboctahedra, or octahedra silver nanoparticles on substrates by Langmuir-Blodgett techniques but their work was focused more on the usage of SERS substrate for detecting arsenic species in water. Therefore, their crystalline structure was not optimized [66].

Murray and colleagues investigated the crystalline phase of binary nanoparticles [67], which is summarized in their review article [68]. Recently, uniform phosphorous nanoparticles with rods, or hexagonal plates as shown in Fig. 8 have been synthesized and assembled into two-dimensional lattice, in which interfacial assembly techniques were applied [69]. Mirkin et al. have also tried to assemble faceted nanoparticles with DNA and measured their assembled structure indirectly using small angle X-ray scattering data [70]. However, according to TEM imags, structures are not regular over large area.

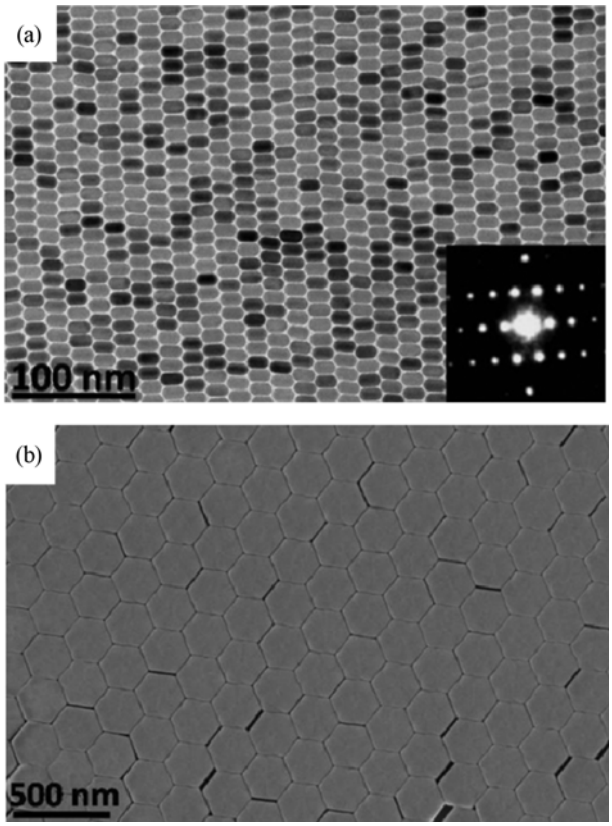

Fig. 8. SEM images of two-dimensional superlattice of (a) $NaYF_4$ nanorods and (b) $NaYF_4$: Yb/Er (20/2 mol%) hexagonal nanoplates [69]. Copyright 2010 National Academy of Sciences, USA.

2. Directional Self-assembly of Particles by Selective Bonding

As shown in Fig. 9, hybrid particles can be functionalized selectively. In case of semiconducting nanorods capped with gold nanoparticles at the tips, we could functionalize metallic particles with thiol compounds [71,72]. Similarly, gold nanorods can be functionalized anisotropically which are stabilized with CTAB on longitudinal side wall and polystyrene at both ends. Therefore, they can be assembled by bonding either end-to-end or side-to-side so that chains or bundles (or sheets) can be formed, respectively (See Fig. 9(a)) [73,74].

In case of hybrid nanoparticles consisting of two different spheres as shown in Scheme 1, those spheres are different in terms of reactivity. Therefore, in the presence of reactive molecules in solution, they can react with reactive molecules. When bifunctional molecules are used such as dithiol, they can be assembled into clusters, in which of cluster configuration can be varied as a function of bond strength between dithiols and nanoparticles and steric hindrance also affected the configurations of clusters as shown in Fig. 9(b) [75]. DNA can be used to bind molecules to form clusters of nanoparticles because it has been used for the clusters of gold nanoparticles [76].

3. Optical Properties of Plasmonic Molecules

The metallic nanostructures composed of multiple building block particles are called *plasmonic molecules*. The optical properties of such plasmonic molecules can be described by the concept of *plas-*

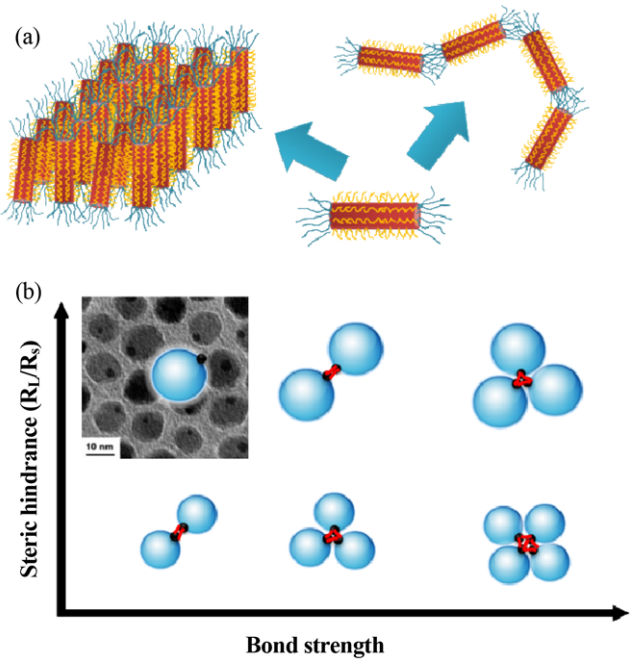

Fig. 9. (a) Schematic of end-to-end or side-to-side assembly of nanorods stabilized with different stabilizers. (b) TEM image of gold-iron oxide hybride nanoparticles [75] and schematics of their clusters, in which their configurations depend on the concentration of dithiols (bond strength) and size ratio (steric hindrance) of gold and iron oxide spheres. Reprinted with permission ref. 75 Copyright 2005 American Chemical Society.

mon hybridization, considering the interaction and hybridization of neighboring surfaces and the plasmon of each nanostructure, finally determining the optical properties of complex metallic nanostrucures [77]. The plasmon hybridization of multiparticle plasmons such as dimers, trimers, and quadramers has been considered by the similar approaches of the hybridization of molecular orbitals, and other structures such as nanoshell plasmons or nanoparticles on a film have been also treated according to this concept.

Besides plasmonic molecules, *plasmonic chains* composed of gold nanorods which are assembled by end-to-end attachements could be also constructed [78]. Gold nanorods were treated with thiol-containing molecules such as MPA (mercaptopropionic acid), which induces interparticle hydrogen bonding between carboxylic acids of MPA molecules. Through this approach, gold nanorods were assembled as plasmonic chains in longitudinal direction in the mixed dispersion medium of water and acetonitrile. The resultant surface plasmon was red-shifted due to *interplasmon coupling*, and similar behavior was observed from the aligned gold nanorods on multiwalled carbon nanotubes (MWCNTs) [79].

CONCLUSION

For unifrom anisotropic nanoparticles including rod-like, disk-like (or platelet), faceted or hybrid nanoparticles, innovative synthetic methods have been devised and unusual optical properties were measured, which are in good agreement with theoretical prediction. Then, inspired by the recent progress in the synthesis and assembly of anisotropic colloids at micrometer scales, research activity at nanoscale has also shifted form isotropic to anisotropic nanoparticles. Particularly, selective modification or overgrowth of anisotropic nanoparticles paves the way for the development of new types of self-assembled nanoarchitectures. Moreover, since those structures have unique optical properties or surface plasmonics, they have many potential applications including sensors, miniaturized optical or electronic devices, photonic curcuits, and medical diagnostics [80-82]. In addition, since metamaterials are nanostructured materials of metallic building blocks, it should be possible to materialize them by assembling anisotropic metallic particles [83].

ACKNOWLEDGEMENT

This work was supported by a research grant of the Chungbuk National University in 2011.

REFERENCES

1. W. U. Huynh, J. J. Dittmer and A. P. Alivisatos, *Science*, **295**, 2425 (2002).
2. S. C. Glotzer and M. J. Solomon, *Nat. Mater.*, **6**, 557 (2007).
3. (a) K. J. Lee, J. Yoon and J. Lahann, *Curr. Opin. Coll. Interface Sci.*, **16**, 195 (2011), (b) S. Mitragotri and J. Lahann, *Nat. Mater.*, **8**, 15 (2009), (c) Andreas Walther and Axel H. E. Müller, *Soft Matter*, **4**, 663 (2008), (d) F. Wurm and A. F. M. Kilbinger, *Angew. Chem. Int. Ed.*, **48**, 8412 (2009), (e) S.-M. Yang, S.-H. Kim, J.-M. Lim and G.-R. Yi, *J. Mater. Chem.*, **18**, 2177 (2008), (f) S. Jiang, Q. Chen, M. Tripathy, E. Luijten, K. S. Schweizer and S. Granick, *Adv. Mater.*, **22**, 1060 (2010), (g) D. Dendukuri and P. S. Doyle, *Adv. Mater.*, **21**, 4071 (2009), (h) A. Perro, S. Reculusa, S. Ravaine, E. Bourgeat-Lami and E. Duguet, *J. Mater. Chem.*, **15**, 3745 (2005).
4. (a) T. Hyeon, *Chem. Commun.*, **8**, 927 (2003), (b) J. Park, J. Joo, S. G. Kwon, Y. Jang and T. Hyeon, *Angew. Chem. Int. Ed.*, **46**, 4630 (2007).
5. (a) T. Sugimoto, X. Zhou and A. Muramatsu, *J. Coll. Interf. Sci.*, **259**, 53 (2003), (b) M. Ocana, M. P. Morales and C. J. Serna, *J. Coll. Inter. Sci.*, **212**, 317 (1999), (c) R. Mendoza-Resendezl, O. Bomati-Miguell, M. PMorales, P. Bonville and C. J. Sernal, *Nanotechnology*, **15**, S254 (2004).
6. S. Sacanna, L. Rossi, B. W. M. Kuipers and A. P. Philipse, *Langmuir*, **22**, 1822 (2006).
7. T. T. Tran and X. Lu, *J. Phys. Chem. C*, **115**, 3638 (2011).
8. Y. Wei, R. Klajn, A. O. Pinchuk and B. A. Grzybowski, *Small*, **4**, 10, 1635 (2008).
9. H. Lee, S. E. Habas, G. A. Somorjai and P. Yang, *J. Am. Chem. Soc.*, **130**, 5406 (2008).
10. H. Gu, R. Zheng, X. Zhang and B. Xu, *J. Am. Chem. Soc.*, **126**, 5664 (2004).
11. T. Teranishi, Y. Inoue, M. Nakaya, Y. Oumi and T. Sano, *J. Am. Chem. Soc.*, **126**, 9914 (2004).
12. H. Yu, M. Chen, P. M. Rice, S. X. Wang, R. L. White and S. Sun, *Nano. Lett.*, **5**, 379 (2005).
13. C. J. Murphy, A. M. Gole, S. E. Hunyadi and C. J. Orendorff, *Inorg. Chem.*, **45**, 7544 (2006).
14. Y. Xia, P. Yang, Y. Sun, Y. Wu, B. Mayers, B. Gates, Y. Yin, F. Kim and H. Yan, *Adv. Mater.*, **15**, 353 (2003).

15. Y.-W. Jun, J.-H. Lee, J.-S. Choi and J. Cheon, *J. Phys. Chem. B*, **109**, 14795 (2005).
16. X. Peng, L. Manna, W. Yang, J. Wickham, E. Scher, A. Kadavanich and A. P. Alivisatos, *Nature*, **404**, 59 (2000).
17. P. D. Cozzoli, L. Manna, M. L. Curri, S. Kudera, C. Giannini, M. Striccoli and A. Agostiano, *Chem. Mater.*, **17**, 1296 (2005).
18. J.-W. Seo, Y.-W. Jun, S. J. Ko and J. Cheon, *J. Phys. Chem. B*, **109**, 5389 (2005).
19. X, Lu, M. Rycenga, S. E. Skrabalak, B. Wiley and Y. Xia, *Annu. Rev. Phys. Chem.*, **60** 167 (2009).
20. J. H. Yu, J. Joo, H. M. Park, S.-I. Baik, Y. W. Kim, S. C. Kim and T. Hyeon, *J. Am. Chem. Soc.*, **127**, 5662 (2005).
21. C. Pacholski, A. Kornowski and H. Weller, *Angew. Chem. Int. Ed.*, **41**, 1188 (2002).
22. N. Du, H. Zhang, B. Chen, X. Ma and D. Yang, *J. Phys. Chem. C*, **111**, 12677 (2007).
23. H. M. Chen, R.-S. Liu, K. Asakura, L.-Y. Jang and J.-F. Lee, *J. Phys. Chem. C*, **111**, 18550 (2007).
24. B. Nikoobakht and M. A. El-Sayed, *Chem. Mater.*, **15**, 1957 (2003).
25. S. Kudera, L. Carbone, M. F. Casula, R. Cingolani, A. Falqui, E. Snoeck, W. J. Parak and L. Manna, *Nano Lett.*, **5**, 445 (2005).
26. (a) T. Mokari, C. G. Sztrum, A. Salant, E. Rabani and U. Banin, *Nat. Mater.*, **4**, 855 (2005), (b) R. Costi, A. E. Saunders, E. Elmalen, A. Salant and U. Banin, *Nano Lett.*, **8**, 637 (2008).
27. P. Li, Z. Wei, T. Wu, Q. Peng and Y. Li, *J. Am. Chem. Soc.*, **133**, 5660 (2011).
28. Y. Xiong, A. R. Siekkinen, J. Wang, Y. Yin, M. J. Kim and Y. Xia, *J. Mater. Chem.*, **17**, 2600 (2007).
29. C. S. Ah, Y. J. Yun, H. J. Park, W.-J. Kim, D. H. Ha and W. S. Yun, *Chem. Mater.*, **17**, 5558 (2005).
30. M. Maillard, P. Huang and L. Brus, *Nano Lett.*, **3**, 1611 (2003).
31. Y. C. Cao, *J. Am. Chem. Soc.*, **124**, 11244 (2002).
32. R. Si, Y.-W. Zhang, L-P. You and C.-H. Yan, *Angew. Chem.*, **117**, 3320 (2005).
33. (a) M. B. Sigman, Jr., A. Ghezelbash, T. Hanrath, A. E. Saunders, F. Lee and B. A. Korgel, *J. Am. Chem. Soc.*, **125**, 16050 (2003), (b) X. Li, H. Shen, J. Niu, S. Li, Y. Zhang, H. Wang and L. S. Li, *J. Am. Chem. Soc.*, **132**, 12778 (2010).
34. C.-C. Chang, H.-L. Wu, C.-H. Kuo and M. H. Huang, *Chem. Mater.*, **20**, 7570 (2008).
35. K.-S. Choi, *Dalton Trans.*, 5432 (2008)
36. C. Li, K. L. Shuford, M. Chen, E. J. Lee and S. O. Cho, *ACS Nano*, **2**, 1760 (2008).
37. A. Tao, P. Sinsermsuksakul and P. Yang, *Angew. Chem. Int. Ed.*, **45**, 4597 (2006).
38. M. Chen, J. Kim, J. P. Liu, H. Fan and S. Sun, *J. Am. Chem. Soc.*, **128**, 7132 (2006).
39. D. Yu and V. W.-W. Yam, *J. Am. Chem. Soc.*, **126**, 13200 (2004).
40. C.-K. Tsung, J. N. Kuhn, W. Huang, C. Aliaga, L.-I. Hung, G. A. Somorjai and P. Yang, *J. Am. Chem. Soc.*, **131**, 5816 (2009).
41. K. Lee, M. Kim and H. Kim, *J. Mater. Chem.*, **20**, 3791 (2010).
42. K. L. Kelly, E. Coronado, L. L. Zhao and G. C. Schatz, *J. Phys. Chem. B*, **107**, 668 (2003).
43. R. Gans, *Ann. Phys.*, **37**, 881 (1912).
44. J. C. M. Garnett, *Philos. Trnas. R. Soc.*, **203**, 385 (1904).
45. D. A. Bruggeman, *Ann. Phys.*, **24**, 636 (1935).
46. L. M. Liz-Marzan, *Langmuir*, **22**, 32 (2006).
47. T. Jensen, L. Kelly, A. Lazarides and G. C. Schatz, *J. Cluster Sci.*, **10**, 295 (1999).
48. L. Novotny, D. W. Pohl and B. Hecht, *Opt. Lett.*, **20**, 970 (1995).
49. R. X. Bian, R. C. Dunn, X. S. Xie and P. T. Leung, *Phys. Rev. Lett.*, **75**, 4772 (1995).
50. P. W. Barber, R. K. Chang and H. Massoudi, *Phys. Rev. B*, **27**, 7251 (1983).
51. B. J. Willy, S. H. Lim, Z.-Y. Li, J. McLellan, A. Siekkinen and Y. Xia, *J. Phys. Chem. B*, **110**, 15666 (2006).
52. C. A. Foss, G. L. Hornyak, J. A. Stockert and C. R. Martin, *J. Phys. Chem.*, **98**, 2963 (1994).
53. M. L. Sandrock, C. D. Pibel, F. M. Geiger and C. A. Foss, *J. Phys. Chem. B*, **103**, 2668 (1999).
54. J. Perez-Juste, L. M. Liz-Marzan, S. Carnie, D. Y. C. Chan and P. Mulvaney, *Adv. Funct. Mater.*, **14**, 571 (2004).
55. S. Link, M. B. Mohamel and M. A. El-Sayed, *J. Phys. Chem. B*, **103**, 3073 (1999).
56. B. J. Wiley, Y. Herricks, Y. Sun and Y. Xia, *Nano Lett.*, **4**, 1733 (2004).
57. S. H. Im, Y. T. Lee, B. Wiley and Y. Xia, *Angew. Chem. Int. Ed.*, **44**, 2154 (2005).
58. B. J. Wiley, Y. Xiong, Z.-Y. Li, Y. Yin and Y. Xia, *Nano Lett.*, **6**, 765 (2006).
59. Y. Sun, B. Mayers, T. Herricks and Y. Xia, *Nano Lett.*, **3**, 955 (2003).
60. B. J. Wiley, Y. Sun and Y. Xia, *Langmuir*, **21**, 8077 (2005).
61. I. Pastoriza-Santos and L. M. Liz-Marzan, *Nano Lett.*, **2**, 903 (2002).
62. L. M. Liz-Marzan, *Langmuir*, **22**, 32 (2006).
63. J.-J. Jiang, Y.-G. Liu, L.-P. Jiang and J.-J. Zhu, *Electrochem. Comm.*, **10**, 355 (2008).
64. A. Gomez-Ramirez, M. T. Lopez-Lopez, J. D. G. Duran and F. Gonzalez-Caballero, *Soft Matter*, 5, 3888 (2009).
65. A. R. Tao, D. P. Ceperley, P Sinsermsuksakul, A. R. Neureuther and P. Yang, *Nano Lett.*, **8**, 4033 (2008).
66. M. Mulvihill, A. Tao, K. Benjauthrit, J. Arnold and P. Yang, *Angew. Chem. Int. Ed.*, **47**, 6456 (2008).
67. (a) J. J. Urban, D. V. Talapin, E. V. Shevchenko, C. R. Kagan and C. B. Murray, *Nat. Mater.*, **6**, 115 (2007), (b) E. V. Shevchenko, D. V. Talapin, N. A. Kotov, S. O'Brien and C. B. Murray, *Nature*, **439**, 55 (2006).
68. S. A. Claridge, A. W. Castleman, Jr., S. N. Khanna, C. B. Murray, A. Sen and P. S. Weiss, *ACS Nano*, **3**, 244 (2009).
69. X, Ye, J. E. Collins, Y. Kang, J. Chen, D. T. N. Chen, A. G. Yodh and C. B. Murray, *Proc. Natl. Acad. Sci. USA*, **107**, 22430 (2010).
70. M. R. Jones, R. J. Macfarlane, B. Lee, J. Zhang, K. L. Young, A. J. Senesi and C. A. Mirkin, *Nat. Mater.*, **9**, 913 (2010).
71. A. Salant, E. Amitay-Sadovsky and U. Banin, *J. Am. Chem. Soc.*, **128**, 10006 (2006).
72. J. L. Baker, A. Widmer-Cooper, M. F. Toney, P. L. Geissler and A. P. Alivisatos, *Nano Lett.*, **10**, 195 (2010).
73. K. Liu, Z. Nie, N. Zhao, W. Li, M. Rubinstein and E. Kumacheva, *Science*, **329**, 197 (2010).
74. Z. Nie, D. Fava, E. Kumacheva, S. Zou, G. C. Walker and M. Rubinstein, *Nat. Mater.*, **6**, 609 (2007).
75. (a) Y. Wei, K. J. M. Bishop, J. Kim, S. Soh and Bartosz A. Grzybowski, *Angew. Chem. Int. Ed.*, **48**, 9477 (2009), (b) H. Yu, M. Chen, P. M. Rice, S. X. Wang, R. L. White and S. Sur, *Nano Lett.*, **5**, 379 (2005).

76. S. J. Tan, M. J. Campolongo, D. Luo and W. Cheng, *Nat. Nanotech.*, **6**, 268 (2011).
77. H. Wang, D. W. Brandl, P. Nordlander and N. J. Halas, *Acc. Chem. Res.*, **40**, 53 (2007).
78. K. G. Thomas, S. Barazzouk, B. I. Ipe, S. T. S. Joseph and P. V. Kamat, *J. Phys. Chem. B*, **108**, 13066 (2004).
79. M. A. Correa-Duarte, J. Perez-Juste, A. Sanchez-Iglesias, M. Giersig and L. M. Liz-Marzan, *Angew. Chem. Int. Ed.*, **44**, 4375 (2005).
80. B. Sun and H. Sirringhaus, *J. Am. Chem. Soc.*, **128**, 16231 (2006).
81. B. Sun and H. Sirringhaus, *Nano Lett.*, **5**, 2408 (2005).
82. B. Sun and H. Sirringhaus, *Nano Lett.*, **8**, 1649 (2008).
83. K. J. Stebe, E. Lewandowski and M. Ghosh, *Science*, **325**, 159 (2009).

Gi-Ra Yi received his BS degree in chemical engineering from Yonsei University, Korea, in 1997 and MS (1999) and PhD (2003) degrees in chemical and biomolecular engineering from KAIST, Korea. He undertook postdoctoral research at the University of California, Santa Barbara, USA, and worked briefly for the Corporate R&D Center of LG Chem Research Park and the Korea Basic Science Institute as a research scientist. In 2009, he joined Chungbuk National University, Korea, as an assistant professor in engineering chemistry. He was a visiting professor at Center for Soft Matter Research in New York University. His current interest is in self-assemblies of colloidal particles at micrometer or nanometer scales, as well as multiphase microfluidics.